

Characteristics of Wind Flow Variation with Wing Development of Space-Reduced Damper

Geun-Uk Baek^{*,**}, Nam-Do Baek^{*}, Myung-Won Lee^{**}, Myungchang Kang^{**,#}

^{*}JEIL Industries, 24, Sinhosandan 3-ro, 87beon-gil, Gangseo-gu, Busan, Republic of Korea

^{**}Graduate school of Convergence Science, Pusan National University, Busan, Republic of Korea

공간축소형 댐퍼의 날개개도에 따른 풍량변화 특성평가

백근욱^{*,**}, 백남도^{*}, 이명원^{**}, 강명창^{**,#}

^{*}제일산업, ^{**}부산대학교 융합학부

(Received 25 March 2021; received in revised form 20 April 2021; accepted 10 June 2021)

ABSTRACT

An experimental device was designed to control the opening of a damper via operating the folding blade drive of the device and to control the amount of air flowing through the damper. In addition, an inverter was installed in the blower to control its fan rotation speed and hence the amount of air flowing through the damper. An experimental study was conducted on the opening of the folding blade damper and changes in the rotational speed of the blower. From the results, the theoretical air volume of the folding blade damper and experimental air volume were observed to be in good agreement within an error range of $\pm 3\%$. As the mass flow rate of the air passing through the folding blade damper increases proportionally with the changes in damper opening and fan rotation speed, the performance of the damper can be controlled proportionally. The mass flow rate was also observed to increase linearly; therefore, the mass flow rate of the air passing through the folding blade damper increases proportionally with changes in the rotation speed of the blower, such that the performance of the damper is proportional to a constant air volume even with varying rotation speeds of the blower.

Key Words : Foldable Blade Damper(접이식 블레이드 댐퍼), Air Volume Change(풍량 변화), Degree of Damper Opening(댐퍼 개도), Number of Revolutions of the Blower(송풍기 회전수), Air Mass Flow Rate(공기 질량 유동율)

1. Introduction

A damper is a device installed in a duct opening

to change the airflow rate. It is not easy to control the airflow rate in this type of damper because the air volume passing through the damper varies depending on the static pressure and degree of opening of the duct. Moreover, it is more difficult to control the airflow rate in a single blade damper

Corresponding Author : kangmc@pusan.ac.kr

Tel: +82-51-510-2361, Fax: +82-51-510-7396

because the airflow rate changes non-linearly according to the degree of the damper opening at the same static pressure^[1,2].

Therefore, multi-blade dampers are used to address the non-linearity issue. In the case of round dampers, it is difficult to use multi-blades. Hence, Venturi-type dampers have been used. In recent years, studies have been conducted on orifice-blade type dampers that have excellent linearity, which is achieved by setting the blades on the orifice neck. Additionally, their characteristics have been comparatively analyzed with those of Venturi-type dampers^[3,4]. However, it is not also easy to control the airflow rate using the orifice-blade type dampers because the pressure changes when the damper opening degree is adjusted^[5]. Originally, Venturi dampers were studied as constant air volume (CAV) dampers, which automatically control airflow rate regardless of pressure changes. However, Venturi dampers have big disadvantages, e.g., the device is complex and the flow resistance is large^[6]. Furthermore, the air volume flowing through the duct is very difficult to block in the damper^[7]. Thus, to block the air volume, an additional device is required. This increases the price of the damper significantly, thereby adding a great burden on the users^[8]. However, there is a trend of using multi-blade dampers to solve the non-linearity problem of dampers^[9].

In mechanical devices, such as engines and combustors that are operated using compressed air in industrial sites, precise dampers are required to supply CAV and provide proportional control according to the change in the damper opening degree. Moreover, conventional plate-type dampers require a large space when the degree of operation is increased. Therefore, research is required to reduce the space occupied by the damper even if the damper opening degree is increased^[10].

Therefore, in this study, we configured the damper such that the damper opening degree can be controlled

by operating a foldable-blade drive unit. Moreover, the proposed damper does not require additional space even if the damper opening degree is increased. Furthermore, the volume and mass flow rates of air passing through the foldable-blade damper increased in proportion to the change in the damper opening degree and the number of rotations (rotations per minute (RPM)) of the blower. Thus, the performance result of the proposed damper showed that CAV was controlled proportionally.

2. Experimental Device and Method

Fig. 1 shows the foldable-blade damper consists of a wind tunnel, foldable-blade drive unit, blower, inverter for controlling airflow rate of the blower, damper, stabilizer, air volume control device, foldable-blade damper opening degree control device, and gas burner-based thermal energy supply device. During operation, the damper opening degree is controlled by operating the foldable-blade drive unit, which controls the air volume flowing into the damper. Furthermore, an inverter was installed to control the fan RPM of the blower to control the air volume flowing into the damper. A stabilizer was installed at the center position of the duct where the air flows into the damper to ensure that the velocity of air flowing through the cross-section inside the duct would be uniform. In brief, the experimental device was set up to achieve CAV and airflow control in proportion to the change in the damper opening degree. Moreover, a thermal energy supply device was installed to control the temperature of the air flowing into the damper. A flowmeter and temperature sensor were installed at the duct outlet to measure the air velocity and temperature, respectively.

Fig. 2 shows the stabilizer installed at the front-end inside the duct of the foldable-blade damper. As the blower is operated, air enters the duct inlet of the foldable-blade damper and passes through the stabilizer, which maintains a constant air

velocity.

Fig. 3 shows the drive unit of the foldable blades, whereas Fig. 4 shows the foldable blades. This study was conducted for a foldable-blade damper that can be applied in a narrow space. Conventional plate-type dampers require a large space when the damper opening degree is increased. However, the foldable-blade damper used in this study requires 50% less space comparatively. Furthermore, conventional damper blades have structures that are difficult to control the air volume passing through the damper as CAV proportional to the static pressure and the degree of opening. To solve these problems, we constructed an experimental foldable-blade damper that facilitates CAV control in proportion to the damper opening degree. We conducted an experimental study using the constructed foldable-blade damper, which can be installed without any spatial constraint by minimizing the space that accommodates the lifting of blades. Precise CAV control was achieved via the horizontal movements of the fluid according to the damper opening degree. The pitch of a foldable blade is 50 mm, and the overall weight of 50 foldable blades, which are 2 mm thick, is 46 kg. The operating speed of the foldable blades was 50 mm/sec, and the torque of the foldable-blade drive axis was set to operate at 1950 kg□m. A drive motor and conveyor technology were used to control the extent of opening and closing of the blades.

Table 1 shows the variables and conditions of the experiment conducted in this study. The experimental variables include the damper opening degree, blower RPM, and hydraulic diameter variation. In the experiment, the damper opening degree was equally divided into ten sections ranging from 10 – 100%, whereas the RPM of the blower was equally divided into seven sections ranging from 172 – 1207 RPM. The hydraulic diameter was divided equally into ten sections ranging from 0.18 – 0.95 m.

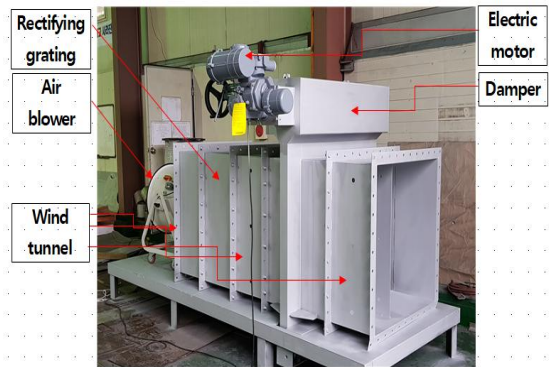


Fig. 1 Experimental apparatus of blade foldable damper

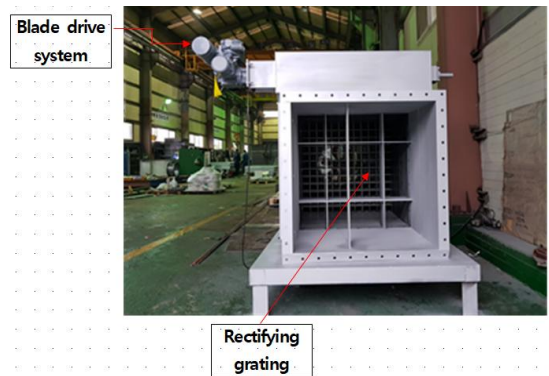


Fig. 2 Rectifying grating of blade foldable damper

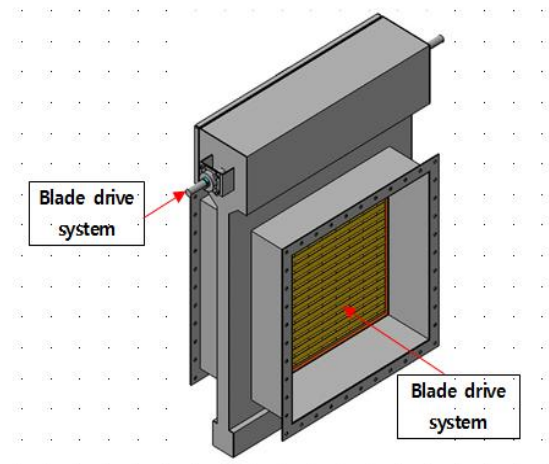


Fig. 3 Driving device of foldable blade

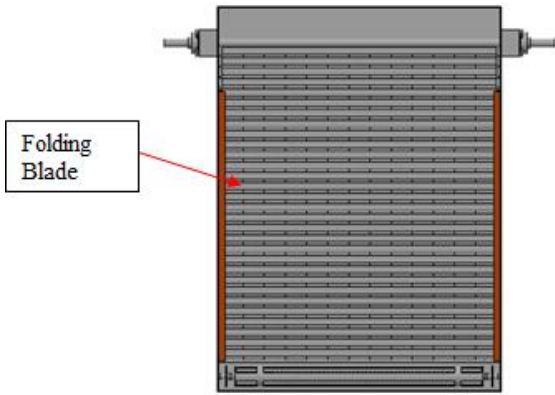


Fig. 4 Foldable blade of blade foldable damper

Table 1 Experimental parameter and conditions

Parameter	Value (unit)
Degree of damper opening	10~100 (%)
Number of Revolutions of the blower	172~1207 (rpm)
Hydraulic diameter	0.18~0.95 (m)

3. Results and Discussion

Fig. 5 shows the change in the theoretical and experimental airflow rates according to the changes in the foldable-blade damper opening degree and blower RPM. Eq. (1) is used to calculate the damper opening degree ϕ .

$$\phi = \frac{A_o}{A_c} \quad (1)$$

where A_c is the cross-sectional area (m^2) of the damper. The length and width of the damper is 1 m. Therefore, the cross-sectional area of the damper is 1 m^2 . A_o represents the cross-sectional area (m^2) after changing the cross-sectional area of the foldable-blade damper. The theoretical airflow rate Q_{air} (m^3/s) was obtained using Eq. (2):

$$Q_{air} = A_c V \quad (2)$$

where V denotes the velocity (m/s) of air flowing in the foldable-blade damper. The experimental airflow rate is the value measured for the air volume supplied by the blower. As shown in Fig. 5, the experiment was conducted by setting the damper opening degree to 60%. The airflow rate of the blower was controlled using the inverter. The blower was maintained at 345, 690, and 1035 RPM, respectively, during the experiment.

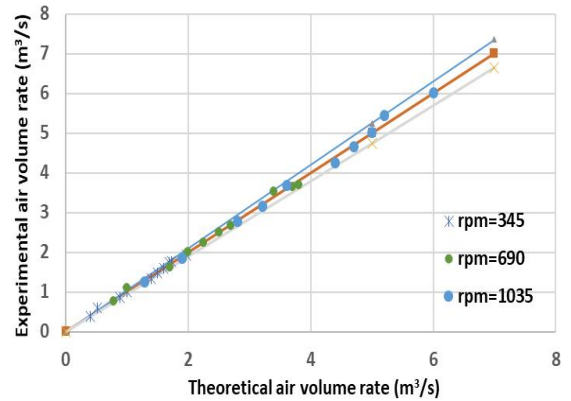


Fig. 5 Accuracy of air flow rate of blade foldable damper

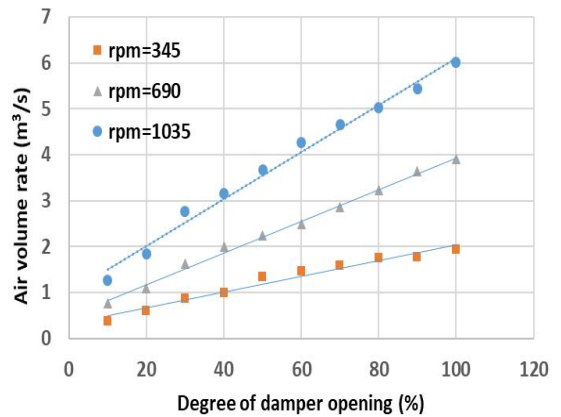


Fig. 6 The rate of change of airflow volume to the change of the open rate of the large perm of the blade folding damper

As shown in Fig. 5, the theoretical and experimental airflow rates coincided well within a range of $\pm 3\%$. Therefore, the accuracy of the experimental result for the change in the airflow rate based on the change in the RPM of the blower of the foldable-blade damper was high.

Fig. 6 shows the change rate of the airflow rate according to the change in the damper opening degree of the foldable-blade damper. The experiment was conducted by dividing the damper opening degree into ten sections ranging from 0 – 100%. As shown in Fig. 6, the air volume flowing into the damper increased linearly as the degree of the damper opening increased. Furthermore, the airflow rate of the blower increased in proportion to the increase in the RPM of the blower. Based on these results, we found that the volume of air passing through the foldable-blade damper increased in proportion to the changes in the damper opening degree and blower RPM, thereby indicating that the proposed damper facilitates proportional control of CAV.

Fig. 7 shows the change rate of the air mass flow rate according to the change in the damper opening degree of the foldable-blade damper. This experiment was conducted by dividing the damper opening degree into ten sections ranging from 0 – 100%. Eq. (3), which is based on the law of conservation of mass, is used to calculate the air mass flow rate \dot{m}_a (kg/s) in the foldable-blade damper:

$$\dot{m}_a = \rho_a A_c V \quad (3)$$

where ρ_c is the air density (kg/m^3), and V is the velocity (m/s) of air flowing through the foldable-blade damper. As shown in Fig. 7, the change rate of the air mass flow rate in the damper increased linearly as the degree of the damper opening increased and in proportion to the increase in the RPM of the blower. Therefore, we found that the change rate of the mass flow rate of the air passing through the foldable-blade

damper increases in proportion to the change in the damper opening degree and the RPM of the blower, thereby indicating that the proposed damper facilitates proportional control of CAV.

Fig. 8 shows the change in the Reynolds number according to the change in the hydraulic diameter of the foldable-blade damper. Eq. (4) defines the wetted perimeter P (m) of the foldable-blade damper:

$$P = 4a \quad (4)$$

where a is the length (m) of a side in the cross-section of the foldable-blade damper.

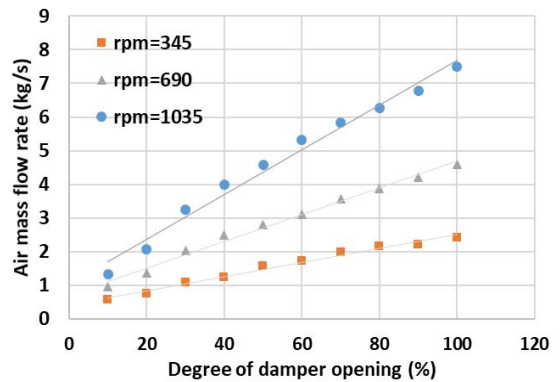


Fig. 7 Air air volume change rate due to the change in the open rate of the blade folding damper

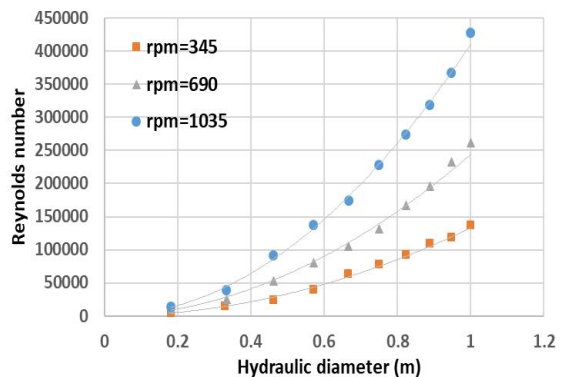


Fig. 8 Changes in reynolds number for change in hydraulic diameter of blade folding damper

Eq. (5) is used to calculate the hydraulic diameter D_h (m).

$$D_h = \frac{4A_c}{P} \quad (5)$$

Eq. (6) is used to calculate the Reynolds number Re_D .

$$Re_D = \frac{\rho_a VA}{\mu} \quad (6)$$

where A denotes the cross-sectional area (m^2) of the damper, and μ denotes the viscosity coefficient ($N \square s/m^2$) of air. Fig. 8 shows the experimental value calculated for the change in the Reynolds number according to the change in the hydraulic diameter under the same experimental conditions, as shown in Fig. 6. As the hydraulic diameter of the damper increased, the Reynolds number increased in proportion to the square of the airflow rate, as shown in Fig. 9. Because the Reynolds number of air passing through the foldable-blade damper increases in proportion to the change in the hydraulic diameter, we concluded that it verifies the reliability of the change in airflow rate in the damper.

Fig. 9 shows the change rate of the airflow rate according to the change in the RPM of the blower in the foldable-blade damper. The experiment was conducted by dividing the RPM of the blower into seven sections ranging from 172 – 1208 RPM. In the experiment, the damper opening degree was set to be 30, 60, and 90%, respectively.

As the RPM of the blower increased, the airflow rate in the damper increased linearly, as shown in Fig. 9. As the flow rate of air passing through the foldable-blade damper increases in proportion to the change in the RPM of the blower, the performance results of this damper suggest that CAV is controlled proportionally, even when the RPM of the blower changes.

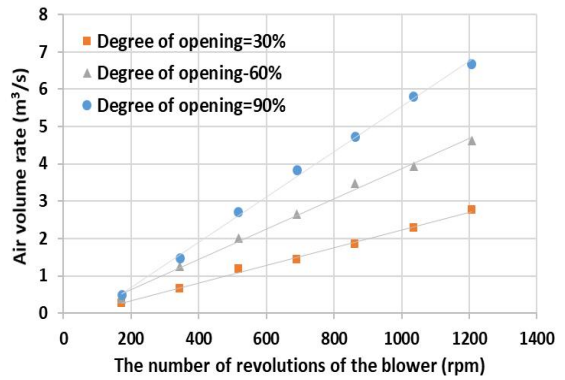


Fig. 9 The rate of change of air flow rate to the change of the rotation speed of the blower in the blade folding damper

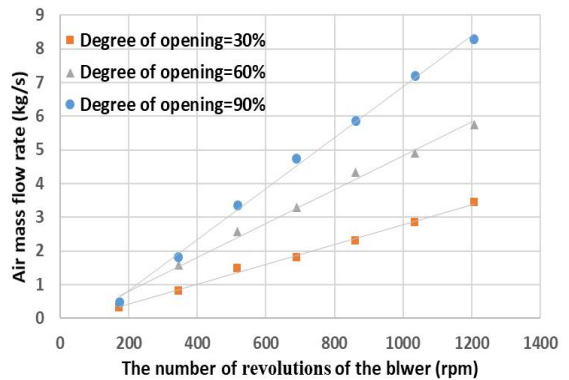


Fig. 10 Changes in mass flow rate of air to changes in the number of rotations of the blower

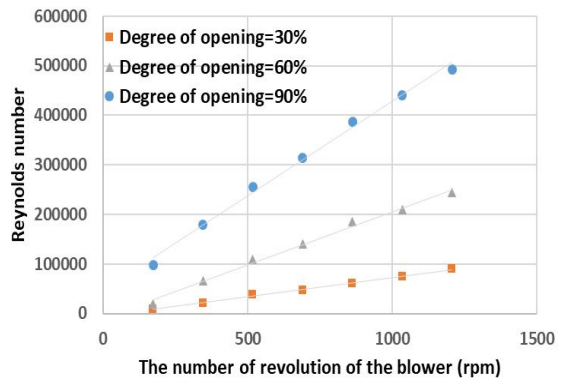


Fig. 11 Change of reynolds number to change of rotation speed of a sung fan

Fig. 10 shows the change in the air mass flow rate according to the change in the RPM of the blower in the foldable-blade damper. In Fig. 10, the experimental value was calculated for the change in the mass flow rate according to the change in the RPM of the blower under the same experimental conditions, as shown in Fig. 9. As the RPM of the blower increased, the mass flow rate of air flowing into the damper increased linearly, as shown in Fig. 10. Because the mass flow rate of air passing through the foldable-blade damper increases in proportion to the change in the RPM of the blower, the performance results of this damper indicate that the CAV is controlled proportionally, even when the RPM of the blower changes.

Fig. 11 shows the change in the Reynolds number according to the change in the RPM of the blower in the foldable-blade damper. The experimental value was calculated for the change in the Reynolds number according to the change in the RPM of the blower under the same experimental conditions, as shown in Fig. 9. The Reynolds number increased linearly in proportion to the increase in the RPM of the blower. As the Reynolds number of air passing through foldable-blade increases in proportion to the increase in the RPM of the blower, we concluded that it verifies the reliability of the change in the airflow rate in the damper. Based on the aforementioned experimental results, we expect that the foldable-blade damper can supply air based on CAV and proportional control to various mechanical systems that use air in industrial sites.

4. Conclusion

We configured a foldable-blade drive unit to control the damper opening degree and conducted a study on a damper that does not require additional space, even when the damper opening degree was increased, to investigate the performance of the

foldable-blade damper. We found that the theoretical and experimental airflow rates of the foldable-blade damper coincided well within a range of $\pm 3\%$. Furthermore, the accuracy of the experimental result was high in terms of the change in the airflow rate based on the changes in the damper opening degree of the foldable-blade damper and RPM of the blower. As the mass flow rate of the air passing through the foldable-blade damper increased in proportion to the changes in the damper opening degree and RPM of the blower, the performance results of this damper showed that CAV is controlled proportionally. As the hydraulic diameter of the damper increased, the Reynolds number increased in proportion to the airflow rate. Because the mass flow rate of the air passing through the foldable-blade damper increased linearly in proportion to the change in the RPM of the blower, the performance results of the damper showed that the CAV was controlled proportionally even when the blower RPM changed.

REFERENCES

1. Vadiialaa, H., Sonib, D. P. and Panchalc, D. G., "Semi-Active Control of a Benchmark Building using Neuro-Inverse Dynamics of MR Damper", *Procedia Engineering*, Vol. 51, pp. 45-54. 2013.
2. Lee, C. B., Cheon, J. S., Kim, S. H., Park, J. Y. and Joo, H. K., "Metal Fuel Development and Verification for Prototype Generation IV Sodium-Cooled Fast Reactor", *Nuclear Engineering and Technology*, Vol. 48, No. 5, pp. 1096~1108, 2016.
3. Yoo, J. W., Chang, J. W., Lim, J. Y., Cheon, J. S., Lee, T. H., Kim, S. K., Lee, K. L. and Joo, H. K., "Overall System Description and Safety Characteristics of Prototype Gen IV Sodium Cooled Fast Reactor in Korea", *Nuclear Engineering and Technology*, Vol. 48, No. 5, pp. 1059~1070. 2016.

4. You, Y. H., Ahn, H. J., "A Passive Reaction Force Compensation (RFC) Mechanism for a Linear Motor Motion Stage", *IJPEM*, Vol. 15, No. 5, pp 1-5, 2014.
5. Lee, H. S., Yoon, K. H., Cheon, J. S. and Lee, C. B., "Integrity Evaluation of Control Rod Assembly for Sodium-Cooled Fast Reactor due to Drop Impact", *Transactions of the Korean Society of Mechanical Engineers A*, Vol. 41, No. 3, pp. 233~239, 2014.
6. Kim, H. S., Seong, M. S., Choi, S. B. and Kwon, O. Y., "Performance Evaluation of a Full Vehicle with Semi-active MR Suspension at Different Tire Pressure", *Transactions of the KSNVE*, Vol. 21, No. 11, pp. 1067~1073. 2011.
7. Lee, G. M., Ju, Y. H. and Park, M. S., "Development of a Low Frequency Shaker using MR Dampers", *International Journal of Precision Engineering and Manufacturing*, Vol. 14, No. 9, pp. 1647~1650, 2013.
8. Seong, M. S., Choi, S. B., Kim, C. H., Lee, H. K., Baek, J. H., Han, H. H. and Woo, J. K., "Experimental Performance Evaluation of MR Damper for Integrated Isolation Mount", *Transactions of the KSNVE*, Vol. 20, No. 12, pp. 1161~1167, 2010.
9. Kim, G. W., Yoon, S. S., Kim, K. C., Lee, M. W. and Kang, M. C. "A Study on the Removal Characteristics of a Radioactively Contaminated Oxide Film from the Irradiated Stainless Steel Surface Using Short Pulsed Laser Ablation", *Journal of the Korean Society of Manufacturing Process Engineers*, Vol. 19, No. 10, pp. 105-110, 2020.
10. Ahn, H. J., You, Y. H., "An Eddy Current Damper for Reaction Force Compensation for a Linear Motor Motion Stage", 14th ISMB, Linz, Austria, Aug. 11-14, 2014.